CHAPTER VI

SOLIDS VISCOSITY MEASUREMENTS IN IN THREE-PHASE FLUIDIZED BED

6.1 Introduction

The thermo-physical properties of three-phase fluidized beds have a major impact on the analysis and design of reactors in the biological, chemical, petroleum, food and pharmaceutical industries. The viscosity is one of these properties.

Viscosity is a measure of the internal friction when one "fluid" layer is made to move relative to another layer. For Newtonian fluids, the viscosity can simply be defined mathematically by the following formula,

$$\tau = \mu \gamma \qquad (6.1)$$

where τ is the shear stress, its unit of measurement is dynes per square centimeter (dynes/cm^2); γ is the shear rate, its unit of measure is called the reciprocal second (sec^{-1}); and μ is the viscosity which has the unit of poise.

In three-phase fluidized beds, the particles can be treated as a continuum with a scale length that is much larger than the particle diameter. The rheological behavior of such continuum results from the cumulative effects of macroscopic (at the length scale of the particle) forces due to interaction between particles and hydrodynamic drag forces. Thus, the gas-liquid-solid mixtures are always more viscous than the liquid from which they are made. Unlike most of Newtonian fluids that are formed as pure substances such as water, multiphase fluids generally behave like non-Newtonian fluids and, as a result,

they do not have a single value for viscosity.

The viscosity measurement of the fluidized bed and its correlation with a glass-forming liquid model was first introduced by Hetzer and Williams (1969), when they analyzed average bed viscosity and expansion for homogeneous, water-fluidized beds of uniform glass spheres having diameters from 32 to 487 μm. A review of experimental studies for the measurements of viscosity in gas-solids fluidized beds is given by Cherimisinoff and Cherimisinoff (1984).

In a three-phase fluidized bed, the rheological behavior of the bed predominantly reflects the granular viscosity of the solids. Gidaspow (1994) expressed this term as:

$$\mu_s = \frac{2\mu_{dil}}{(1+e)\,g_o}\left[1+\frac{4}{5}(1+e)\,g_0\epsilon_s\right]^2+\frac{4}{5}\epsilon_s^2\rho_s d_p(1+e)\,g_o\left(\frac{\Theta_s}{\pi}\right)^{\frac{1}{2}} \qquad (6.2)$$

Dilute Phase Viscosity :

$$\mu_{dil} = \frac{5\sqrt{\pi}}{96}\rho_s d_p\sqrt{\Theta_s} \qquad (6.3)$$

and Radial Distribution Function,

$$g_o = \left[1-\left(\frac{\epsilon_s}{\epsilon_{s,max}}\right)^{\frac{1}{3}}\right]^{-1} \qquad (6.4)$$

where Θ_s is granular temperature that can be obtained from the kinetic oscillation energy balance. It is apparent from the above expression that the particle size, density and packing also affect bed rheology.

Song and Fan (1986) expressed the viscosity of three-phase fluidized bed as "apparent" (or effective) overall viscosity, which is due to the viscosities of the gas and

liquid phases, particle-particle interactions, and bed expansion. This "apparent" (or effective) viscosity for a homogeneous three-phase fluidized bed is defined as,

$$\mu_{bed} = \epsilon_g \mu_g + \epsilon_l \mu_l + \mu_s \qquad (6.5)$$

They found that the bed voidage and gas flow rate are important factors in the three-phase fluidized bed. It is also observed in this experiment that the bed voidage is influenced by the gas and liquid flow rates, and the fluctuations in "apparent" bed viscosity correlate with the bed voidage.

The objective of this chapter is focused on the measurement of viscosity of three-phase fluidized bed under actual operating conditions, using a simple viscometric flow generated by a vertical rotating cylinder. Thus the measured viscosities would be close to those required in the hydrodynamic analysis. In addition, some experiments are conducted in the two-phase fluidized bed as well.

6.2 Experimental Setup and Procedure

The experimental setup consisted of two major parts : the fluidization equipment, and a Brookfield viscometer. A schematic of the experimental setup is shown in Figure 6.1.

6.2.1 Fluidization Equipment. The experiment was conducted in a vertical plexiglas column of 30.48 cm width, 213.36 cm height and 5.08 cm breadth. The bottom of the column (or bed) consisted of gas and liquid distributors. The liquid was pumped to the bed through a 1.0 inch (2.54 cm) I.D. stainless steel pipe, located at the bottom of the bed. The liquid was distributed by two perforated plexiglas plates with many 0.277 cm diameter holes. They were placed at 35.56 cm and 50.8 cm above the bottom of the

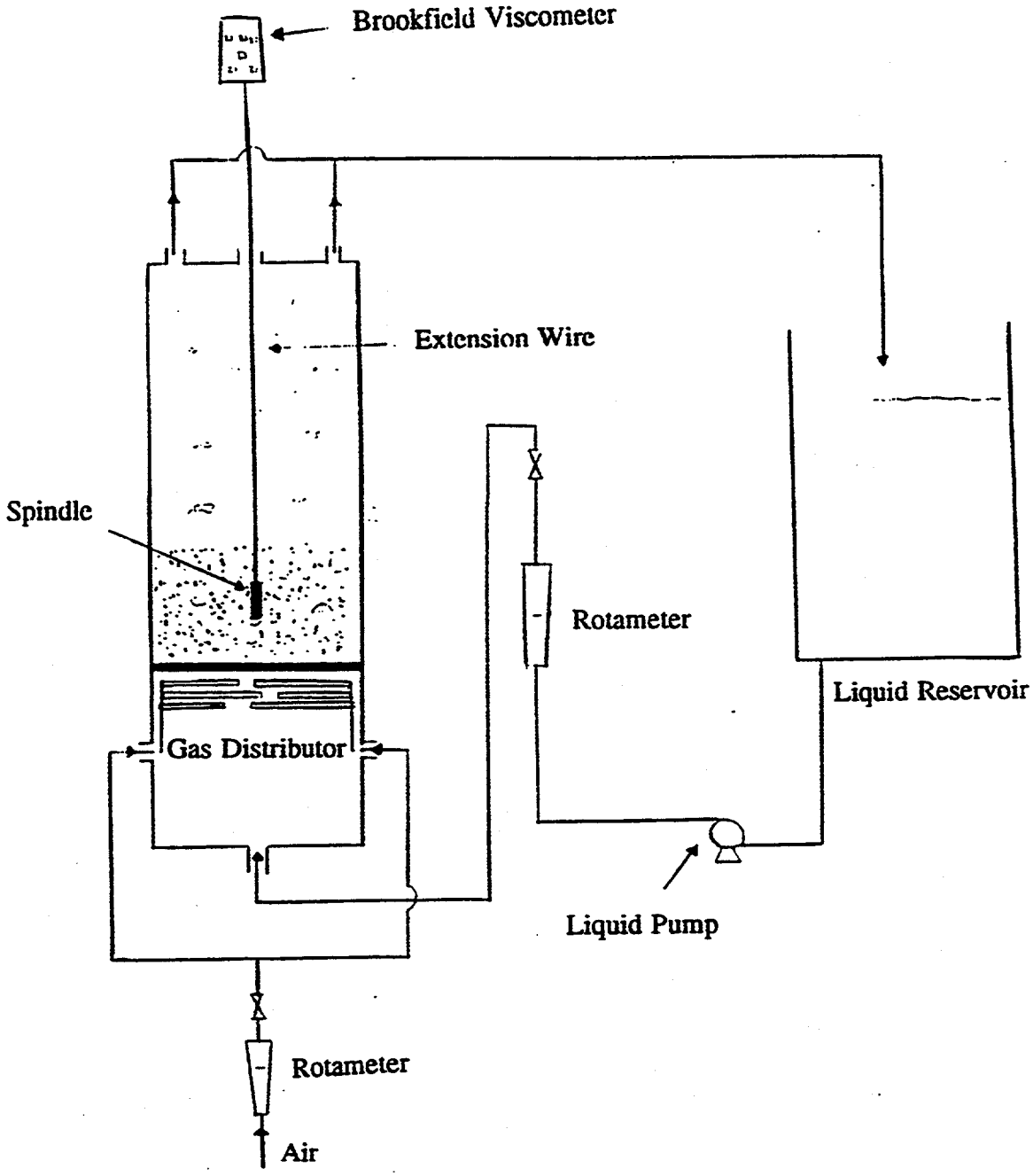

Figure 6.1. Schematic Diagram of the Experimental Apparatus

bed. The gas was distributed to the bed through six staggered tubes with fine pores of 41.88 μm diameters. The gas distribution tubes were located between the perforated plexiglas plates.

6.2.2 Brookfield Viscometer. A Brookfield digital viscometer (model LVDV-II+) with spring torque of 673.7 dyne-cm was used to measure the effective bed viscosities in this experiment. This viscometer can produce twenty different rotational speeds ranging from 0 to 100 revolutions per minute (rpm) at four different modes, namely, LV, RV, HA, and HBDVII+. The viscometer readings were recorded with a Hewlett-Packard (HP) LaserJet series II printer.

6.2.3 Experimental Procedure. The liquid from the storage tank was fed to the bottom of the bed using a centrifugal pump. The gas was fed to the bed through a compressor. The viscometer was placed at the top of the bed, and secured over the centerline of the bed. A cylindrical spindle (#1 LV) of 0.9421 cm diameter, 7.493 cm effective length and overall height of 11.50 cm was used. The cylindrical spindle was attached to the bottom of the viscometer without the guard and was lowered inside the fluidized bed by an extension wire until it was completely immersed in the three-phase mixture.

Air and water were used as the gas and liquid, respectively, in this experiment. Ballotini (leaded glass beads) with a diameter of 800 μm and a particle density of 2.94 g/cm^3 were used as the solids. A constant superficial gas velocity of 3.364 cm/sec was used throughout the experiment, while the superficial liquid velocities were varied between two different values, 2.037 cm/sec and 4.037 cm/sec. The experiments were

conducted at a temperature of 20°C.

The measurements in this experiment were made under LV mode at six different speeds consisting of 2, 4, 6, 10, 12 and 20 rpm. At each rotational speed, between 10 and 30 readings were taken. The calibration of the viscometer-spindle apparatus was done using a Newtonian liquid, namely, water.

The bed expansion measurements were made by visual observation of the height of the bed's upper surface at two different liquid velocities as compared to the initial (close-packed) bed height. The bed void fraction was calculated by the following relation (Kim, et al., 1972) :

$$(\epsilon_l)_{u_g} - \epsilon_l = 0.0025\left(Fr_l \frac{\rho_s}{\rho_l}\right)^{0.149}\left(Fr_g \frac{\rho_s}{\rho_g}\right)^{0.161}(Re_l Re_g)^{0.259} \qquad (6.6)$$

where

$$(\epsilon_l)_{u_g} = 0.409\left(Fr_l \frac{\rho_s}{\rho_l}\right)^{0.193} Re_l^{0.074} \qquad (6.7)$$

$$Fr_k = \frac{u_k^2}{g d_p} \qquad k = l,\ g \qquad (6.8)$$

$$Re_k = \frac{u_k d_p \rho_k}{\mu_k} \qquad k = l,\ g \qquad (6.9)$$

6.3 "Apparent" Bed Viscosity

Figure 6.2 shows the "apparent" bed viscosity as a function of spindle rotation rate (rpm) at two different superficial liquid velocities. As expected, the "apparent" bed viscosity at low liquid flow rate is higher than that at high liquid flow rate for a constant

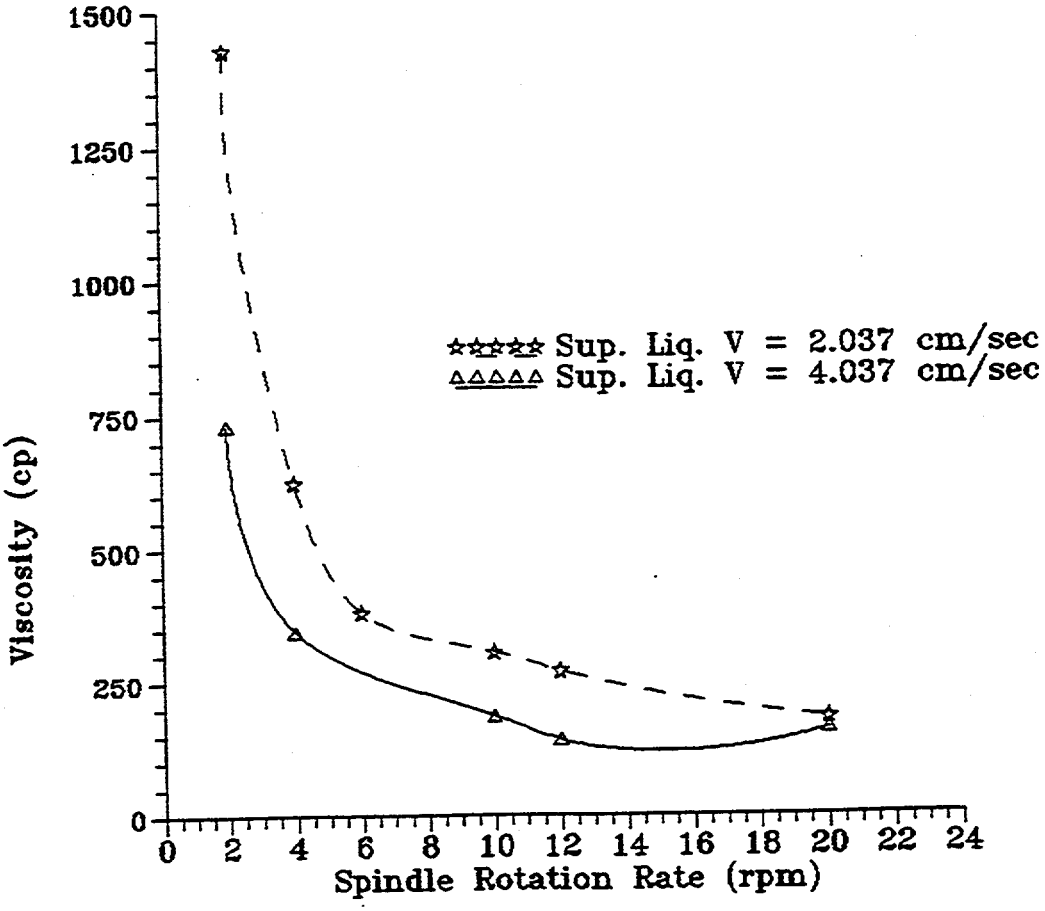

Figure 6.2. Experimentally Measured Viscosity (cp) Versus Spindle Rotation Rate for Three Phase Fluidized Bed (solid Dia =800 micron, Sup Gas Velo. = 3.36 cm/sec)

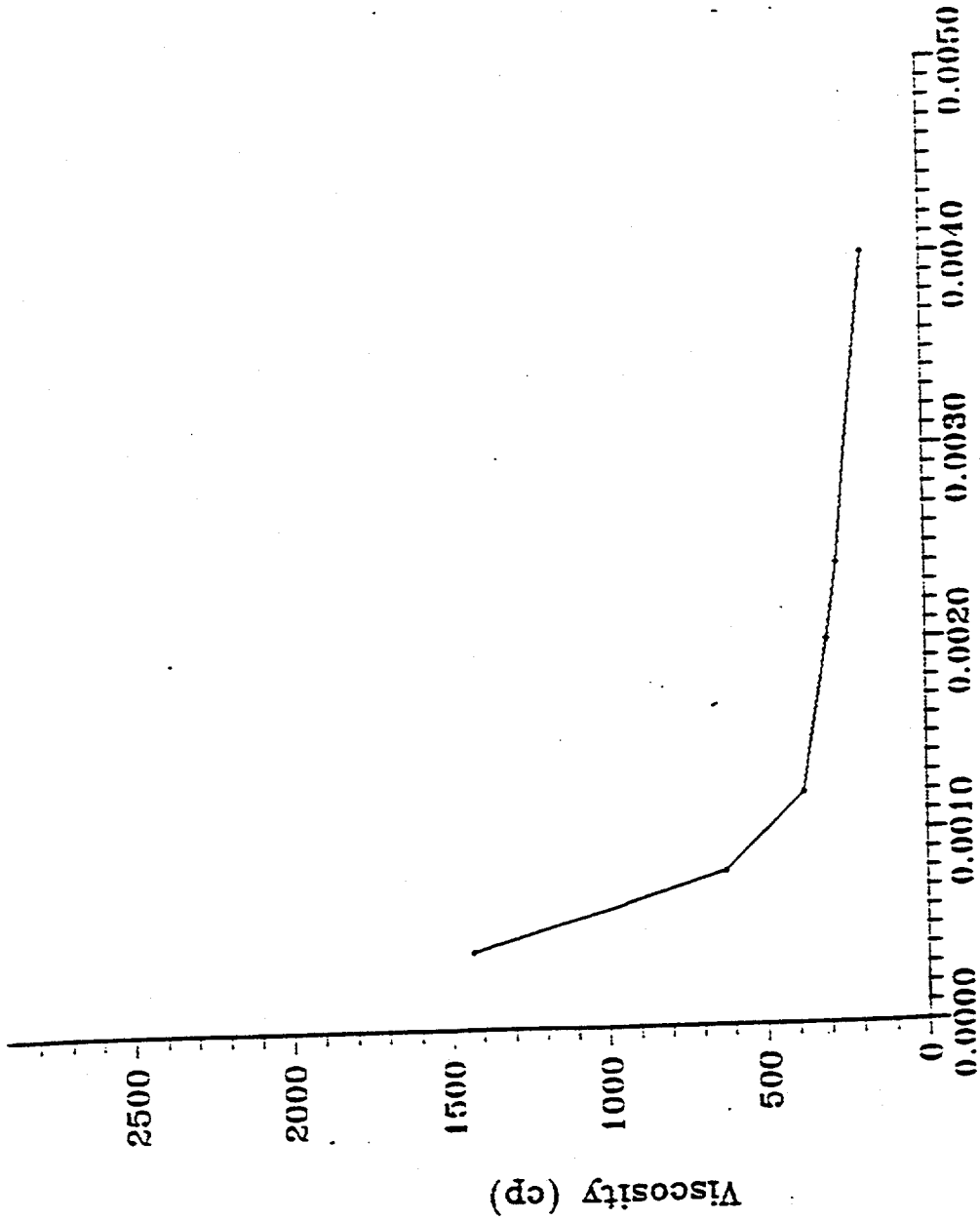

Figure 6.3. Experimentally Measured Viscosity Vs. Shear Rate

spindle rotation rate. This effect is directly related to the solid concentration in the bed. As more liquid is distributed in the bed at a constant gas flow rate, the more dilute the three-phase fluidized bed becomes. The "apparent" bed viscosity as a function of shear rate is shown in Figure 6.3. This figure shows that the "apparent" bed viscosity decreases as the shear rate is increased.

A few of the reasonable causes for a decrease in "apparent" viscosity with increasing spindle rotation rate or shear rate are the following:

(a) centrifugal forces acting on particles close to spindle surface, as well as shear induced migration resulting in less interaction between particles and the spindle; and

(b) a Bingham plastic like behavior of the three-phase fluidized mixture.

The ratio of centrifugal force and gravity force acting on a particle is,

$$\frac{F_{centrifugal}}{F_{gravity}} = \frac{\omega^2 R}{g} \qquad (6.10)$$

where, R is spindle radius and ω is spindle rotation rate. For a spindle diameter of 0.9421 cm and, at the maximum spindle rotation rate of 20 rpm used in the experiment, the above ratio is 0.004. Thus, the effect of centrifugal force on bed viscosity is small at low spindle rotation rate only.

It is difficult to measure solids concentration in the vicinity of spindle surface. Thus, the effect of shear induced migration on "apparent" viscosity is difficult to predict. A measurement technique which does not cause the solids segregation may permit better viscosity measurement. The effect of solid segregation can be reduced numerically by extrapolating the measured "apparent" bed viscosities at moderate shear rates to zero shear

rate as shown in Table 6.1 below. In this table, the liquid volume fractions are calculated from Kims's correlation (Kim, et al., 1972) shown in equations (6.6) to (6.9) and solid volume fractions are calculated from visually measured expanded bed heights under fluidizing conditions. Thus the reported volume fractions are averaged values.

TABLE 6.1 "Apparent" Bed Viscosity

Sup. Gas Velocity (cm/s)	Sup. Liq. Velocity (cm/s)	Bed Volume Fractions Gas	Liquid	Solid	"Apparent" Bed Viscosity at zero shear rate (poise)
3.364	2.037	0.314	0.340	0.346	4.1
3.364	4.027	0.263	0.465	0.272	2.2

The experiments were also conducted in a fluidized bed with a central jet with 1.0 mm diameter particles, and different liquid velocities for liquid-solid fluidization. A description of the fluidized bed with central jet is given in Chapter 5. Figures 6.4 and 6.5 show the transient viscosity measurement readings at a speed of 6 rpm for a fluidized bed with uniform distributer and a fluidized bed with central jet, respectively. The fluctuations in the measurements are a result of change in the volume fractions of gas, liquid and solid phases in the fluidized state. In theory, the frequency of these fluctuations can be analyzed using power spectra techniques and correlated with the frequency of porosity fluctuations in the bed.

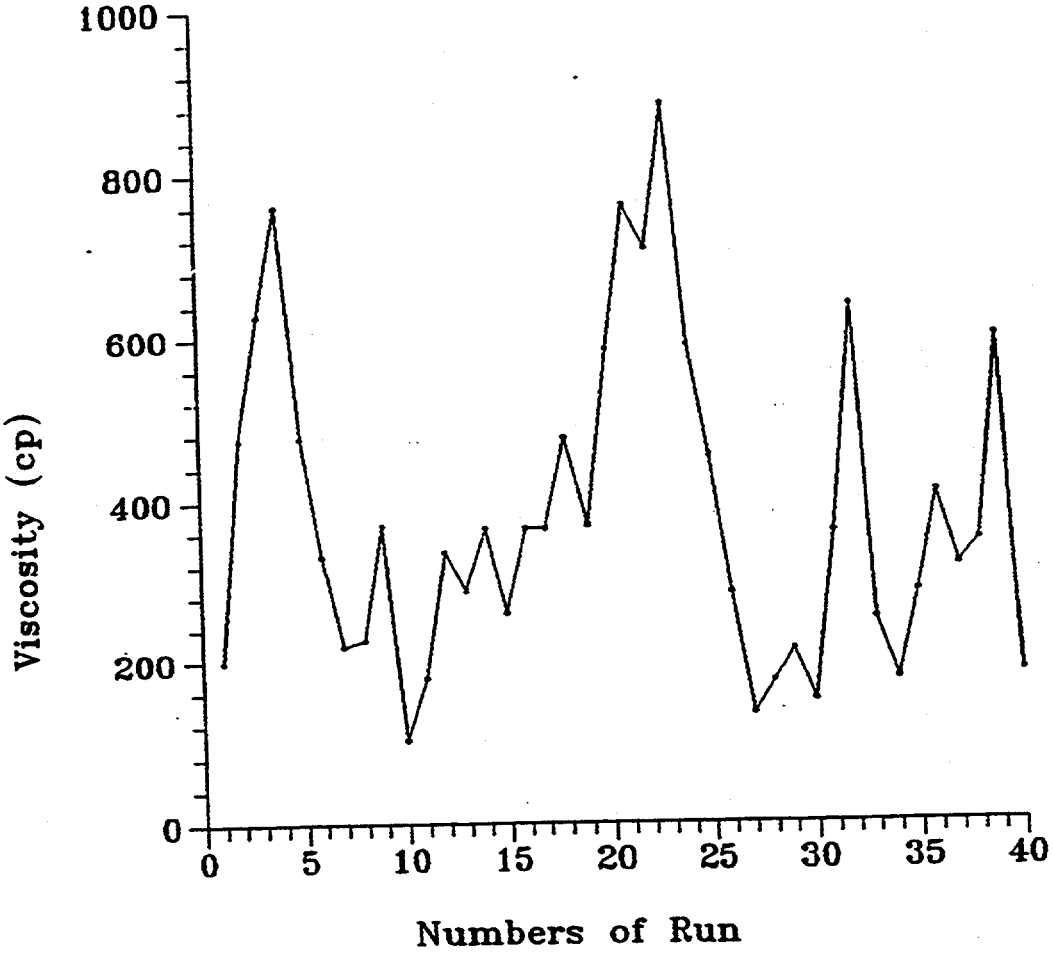

Figure 6.4. Experimentally Measured Viscosity Vs. Numbers of Run for Spindle Rotation Rate of 6 rpm for Three-Phase Fluidized Bed with Uniform Distributer (Solid Dia. = 0.08 mm)

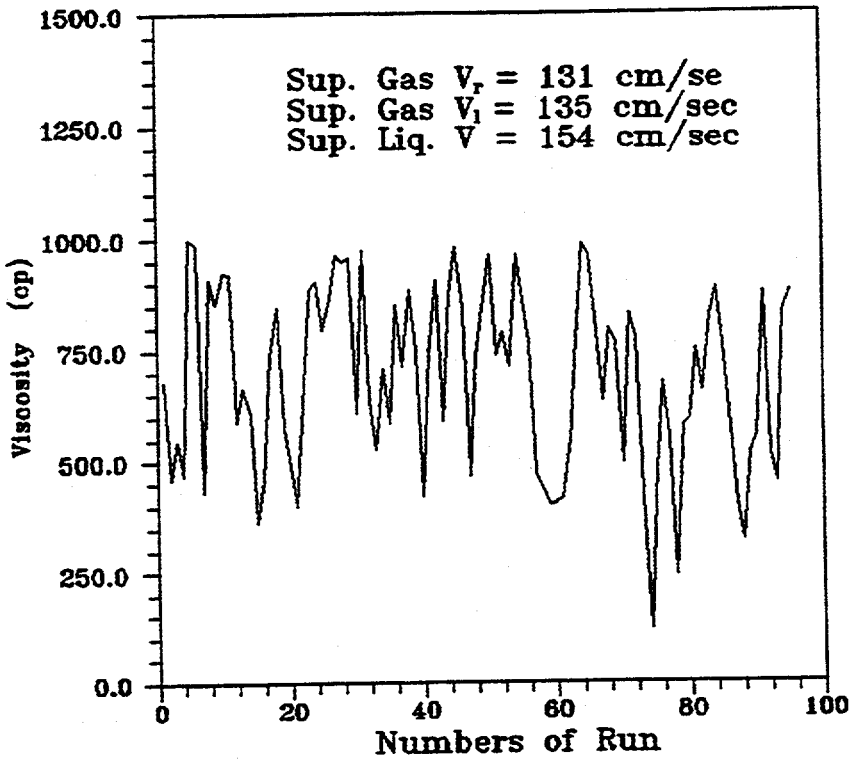

Figure 6.5. Experimentally Measured Viscosity Vs. Numbers of Run for Spindle Rotation Rate of 6 rpm for Three-Phase Fluidized Bed with Central Jet (Solid Dia. = 1 mm)

6.4 Shear Stress Analysis

For analysis of the behavior of a Bingham fluid, consider a cylinder of radius R rotating at an angular velocity ω in a non-Newtonian fluid. In the momentum equation, we make an assumption that the cylinder radius is large as compared to the fluid shear layer and thus there is a uni-directional flow, $v_x(y)$, and no pressure gradient in the x-direction. Neglecting effects of two side walls of the bed, end effects and assuming the Couette flow, this yields

$$\frac{d\tau_{yx}(y)}{dy}=0 \tag{6.11}$$

The constitutive equation for Bingham plastic is,

$$\begin{aligned} \tau_{yx} &= -\mu\frac{dv_x}{dy}+\tau_0 \qquad \tau_{yx} \geq \tau_0 \\ \frac{dv_x}{dy} &= 0 \qquad\qquad\qquad \tau_{yx} < \tau_0 \end{aligned} \tag{6.12}$$

where τ_0 is the yield stress. The yield stress defines a shear layer inside in which the shear stress is greater that the yield stress.

The boundary conditions are the no-slip conditions at both the cylinder surface and at the boundary of shear layer,

$$\begin{aligned} v_x(y=0) &= v_0=\omega R \\ v_x(y=L) &= 0 \end{aligned} \tag{6.13}$$

The solution to equation (6.11) is a linear velocity profile in the shear layer,

$$v_x(y)=v_0\left(1-\frac{y}{L}\right) \tag{6.14}$$

The shear stress at the cylinder surface can be written both in terms of effective bed viscosity (μ) and "apparent" bed viscosity (μ_a) as,

$$\tau_{yx}(R) = \mu\omega\frac{R}{L} + \tau_0 = \mu_a\omega\frac{R}{L} \qquad (6.15)$$

Thus, the "apparent" bed viscosity in terms of effective bed viscosity, yield stress and cylinder rotation rate can be written as,

$$\mu_a = \mu + \frac{\tau_0 L}{\omega R} \qquad (6.16)$$

The angular velocity ω is related to revolutions per seconds (rps) of the cylinder (n), by a simple relation $\omega = 2\,\pi\,n$. The equation (6.16) suggests that for a Bingham fluid, "apparent" viscosity is a linear function of the inverse of the cylinder rotation rate.

Figure 6.6 shows a graph of the experimentally measured "apparent" bed viscosity as a function of inverse of spindle rotation speeds. This figure is a variation of Figure 6.2. A good straight line fit of "apparent" bed viscosity can be clearly seen at two different liquid flow rates. Thus, it is evident that the fluidized bed is behaving like a Bingham fluid (Bird, Stewart and Lightfoot, 1960).

Figure 6.7 shows the result for "apparent" viscosity versus the inverse of spindle rotation rates in a two phase fluidized bed. Again, a good straight line fit illustrates that the liquid-solid fluidized bed acts like a Bingham fluid.

6.5 Granular Temperatures in Three-Phase Fluidized Beds

Based on the values shown in Figure 6.2, and equations (6.2) to (6.5), the granular temperatures were calculated from measured bed viscosities.

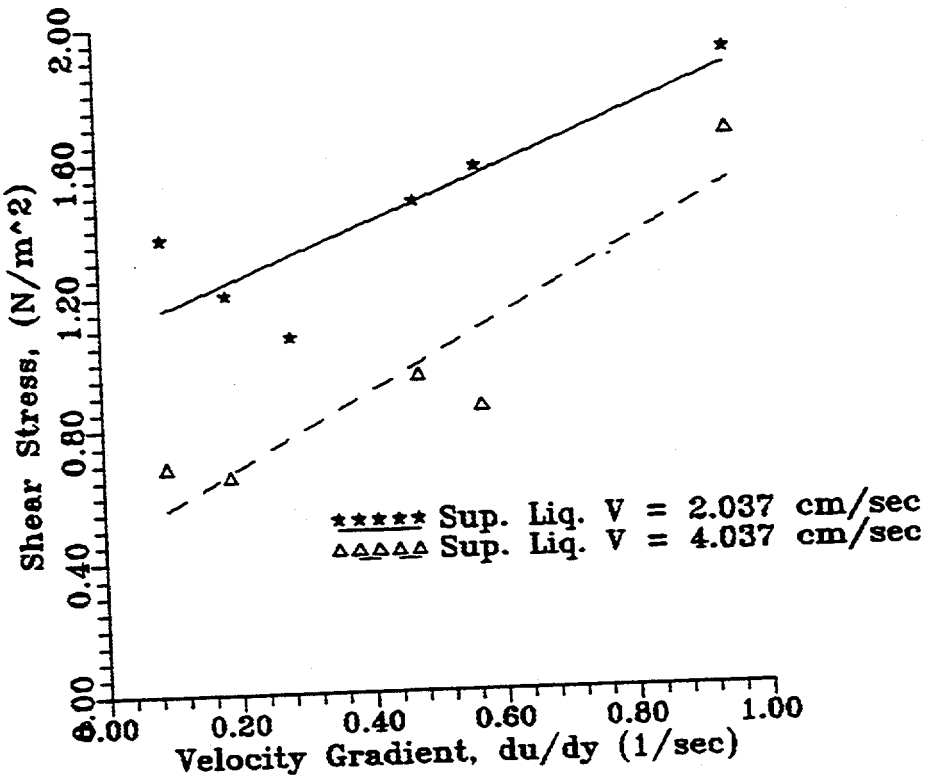

Figure 6.6. Experimentally Measured Shear Stress Vs. Velocity Gradient for Three-Phase Fluidized Bed (Solid Dia. = 0.08 mm, Sup. Gas Velo. = 3.364 cm/sec)

The granular temperatures were calculated to be in the range of 95 to 500 $(cm/sec)^2$ for spindle rotation rates of 6 to 20 rpm. However, at lower spindle rotation rates of 2 to 4 rpm, the calculated granular temperatures were in the range of 1000 to 5000 $(cm/sec)^2$.

The mean fluctuating velocity of particles <C> is related to the granular temperature as,

$$<C> = \sqrt{3\Theta} \qquad (6.17)$$

Thus, at high spindle rotation rates of 6 to 20 rpm, the fluctuating velocity is in the range of 17 to 39 cm/sec (0.17 to 0.39 m/s); whereas, at spindle rotation rates of 2 to 4 rpm, the fluctuating velocities are in the range of 55 to 122 cm/sec (0.55 to 1.22 m/s).

Typical values of the fluctuating velocities for gas-solid fluidized beds were computed by Ding and Gidaspow (1990) to be in the range of 0.17 to 1.7 m/s. Also, based on solids discharge rates from mass flow hoppers, Gidaspow et al. (1986) obtained critical granular velocities in the range of 56.39 to 113.49 cm/sec (0.5639 to 1.1349 m/s) for 86 to 1550 μm size glass beads and 105.19 cm/sec (1.0519 m/s) for 603 μm sized sand particles.

The mean fluctuating velocities obtained from bed viscosity measurements using a Brookfield viscometer are very close to those reported in Chapter 5 based on the direct velocity measurement experiments. Figures 6.8 and 6.9 show the comparison of the measured viscosity with the Brookfield viscometer and calculated solids viscosity from granular temperature using kinetic theory by direct measurement of solids velocity using a high resolution micro image/measuring system technique. In Figure 6.8 the data for

gas-liquid-solid and liquid-solid are continuing with respect to the solid volume fraction. Also, these figures show there is reasonable agreement between the two technique, mostly in the region with a higher concentration of solids.

6.6 Conclusion

1. The role of the Brookfield viscometer in the direct measurement of apparent bed viscosity and the indirect measurement of granular temperatures or fluctuating velocities in fluidized beds is important, in spite of the limitations imposed because of volume fraction fluctuations, axial velocities, transient radial velocity profile, and degree of turbulence, the multiple phases are in contact with spindle.

2. Good agreement between solids viscosities obtained by using two different and independent measurement techniques suggests that the particles collision is an important mechanism in granular flows. This validation of the central mechanism of the kinetic theory of granular flows has far-reaching consequences. The kinetic theory of granular flows can provide an estimation of the rheological properties of multiphase mixtures. Such rheological properties are important for the modeling of the hydrodynamics of fluidized bed reactors and pneumatic transport.

3. In both two-phase and three-phase fluidized beds the predictions of the Bingham fluid match the experimental data reasonably well.

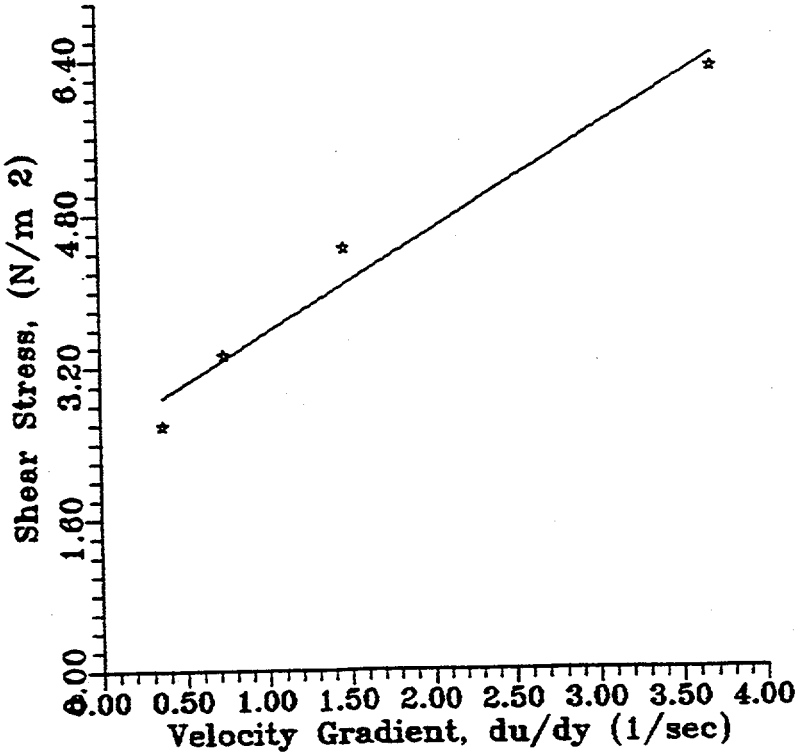

Figure 6.7. Experimentally Measured Shear Stress Vs. Velocity Gradient for Two-Phase Fluidized Bed (Solid Dia. = 1 mm, Sup. Gas Velo. = 332 cm/sec)

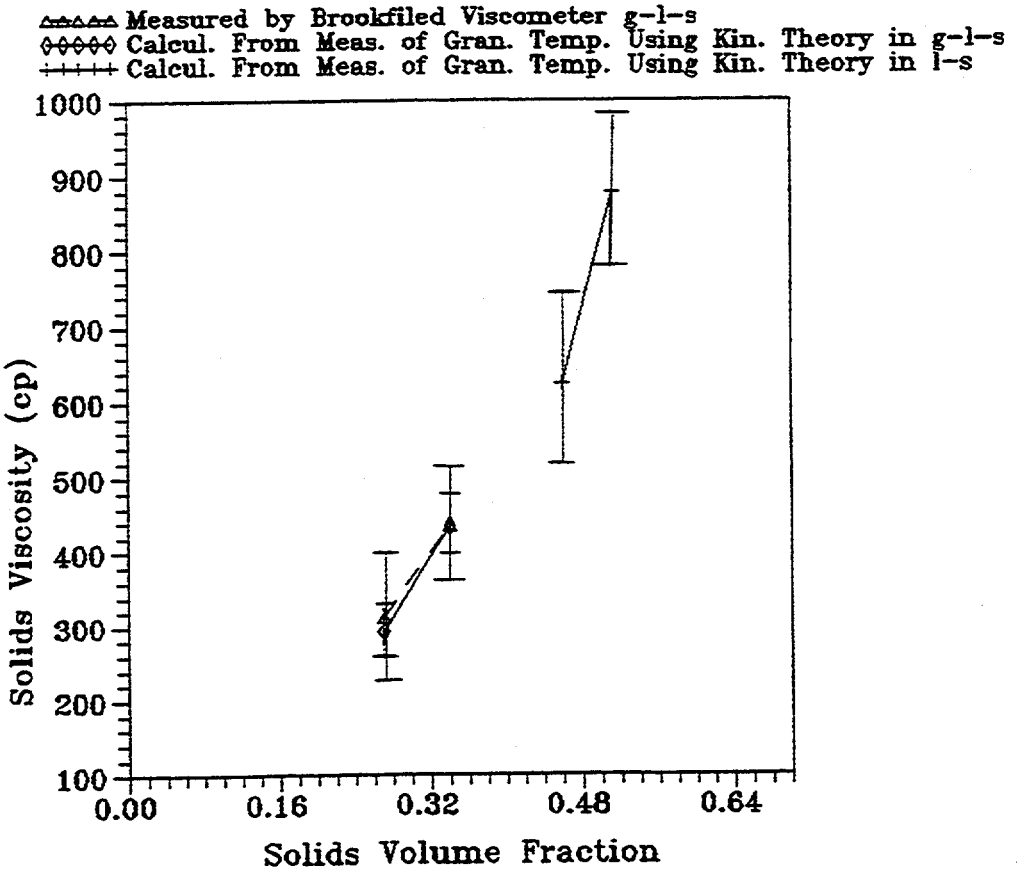

Figure 6.8. Comparison of Measured and Calculated Solid Viscosity In Fluidized Bed

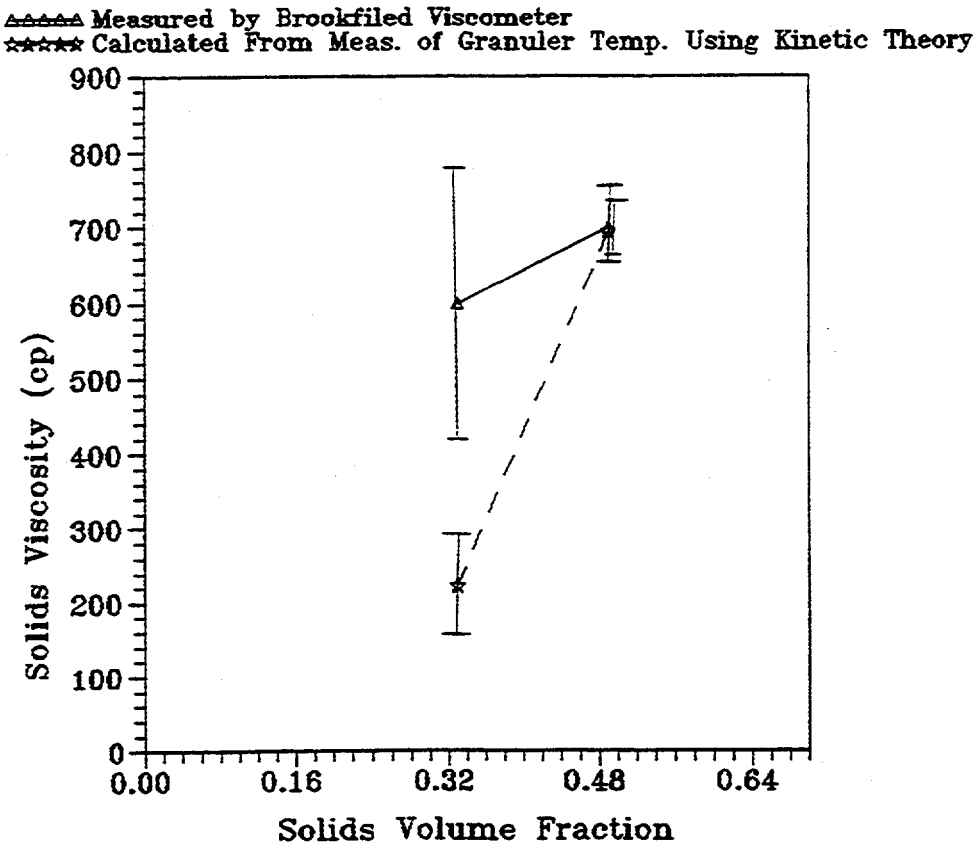

Figure 6.9. Comparison of Measured and Calculated Solid Viscosity In Fluidized Bed with Central Jet